The International Journal of Advanced Manufacturing Technology
https://doi.org/10.1007/s00170-018-1752-0

ORIGINAL ARTICLE

Heat treatment of AA 6082 T6 aluminum alloy coated with thin Al_2O_3 layer by fluidized bed

G. Rubino[1] · F. Trovalusci[2] · M. Barletta[3] · P. Fanelli[1]

Received: 29 September 2017 / Accepted: 7 February 2018

Abstract
Fluidized bed (FB) coating process was used to deposit Al_2O_3 on aluminum substrates to improve, according to previous studies, the overall mechanical and tribological performance of the underlying Al alloys. Fluidized bed coating allowed achieving a compact and dense layer of Al_2O_3 fragments, embedded in the outermost layer of the softer aluminum substrates, through an ambient temperature process. In this framework, this work focuses on the effect of a thermal post-treatment of the Al_2O_3 coating varying the post-treatment temperature and time with the aim of further consolidating the ceramic overlying coating. The high temperature of the thermal post-treatment promoted a diffusion mechanism of the Al_2O_3 fragments that led to further increments in the mechanical and tribological properties of the aluminum substrates. In this respect, morphology, hardness, corrosion, scratch, and wear resistance of the resulting coatings were investigated. The FB coating process and thermal post-treatment have proven to be suitable for the achievement of a good-looking and well-adhered Al_2O_3 protective layer, with mechanical and tribological properties that result in highly enhanced aluminum substrates.

Keywords Fluidized bed (FB) · Aluminum alloy · Al_2O_3 coatings · Heat treatment

1 Introduction

Fluidized beds are well-known manufacturing systems, broadly involved in several industrial domains. Among the large variety of processes that might be run by fluidized beds, powder coating processes are of utmost interest, especially because of the possibility to coat components with highly complex shapes, through easy-to-control and automate process. In particular, fluidized bed (FB) systems provide a response to the growing interest in the deposition of coatings able to get prolonged lifetime, improved hardness, high wear resistance, reduced friction, enhanced corrosion resistance, or the establishment of a diffusion and oxidation barrier on metal substrates [1].

✉ F. Trovalusci
federica.trovalusci@uniroma2.it

[1] Università della Tuscia, DEIM, Largo dell'Università, 01100 Viterbo, Italy

[2] Dipartimento di Ingegneria dell'Impresa, Università degli Studi di Roma "Tor Vergata", via del Politecnico 1, 00133 Roma, Italy

[3] Dipartimento di Ingegneria, Università degli Studi di Roma Tre, via Vito Volterra 62, 00146 Roma, Italy

Recently, new solutions to manufacture single or multilayered coatings able to prevent or retard corrosion of metal structures by conjugating the advantage of the metallic and organic coatings have been proposed, benefiting from the use of FB for the deposition of metallic powders [2]. Scientific literature shows that fluidized bed (FB) technology has been successfully used to deposit hard and corrosion-resistant coatings on ferrous and nonferrous alloys [3]. It is a well-established technology to apply protective coatings on metals such as aluminum alloys, which arouse great industrial impact due to their mechanical characteristics, as, to mention one, the high ratio strength-to-density. In contrast, aluminum alloys is characterized by an often mediocre tribological behavior that limits their applications, whereas the sliding contact is required. Hence, the application on aluminum alloys of protective and wear-resistant coatings is of great practical interest [4–6].

At present, ceramic materials are one of the most reliable candidates for hard protective coatings because of their wear and corrosion resistance. In particular, the high mechanical, chemical, and electrical properties of alumina suggest the use of Al_2O_3 films for several coating applications [7, 8]. Al_2O_3 films can be deposited on Al substrates by several techniques such as sol-gel, PVD, CVD, conventional and hard anodizing, high-velocity, and

Published online: 24 February 2018

plasma-spray processes [9–12]. Nevertheless, these techniques require the use of chemicals to be disposed of, or high-cost and time-consuming equipment, and the need to manage potentially hazardous exhaust emissions. Alternatively, the FB coating process can be performed allowing many advantages, such as environmental safety, feasibility on complex geometries, and the possibility of using basic equipment, which can be easily scaled-up and fully automated for mass production. Further advantages include the potentiality to build multifunctional composite coatings, which may have several purposes including thermal insulation [13]. At the same time, stringent requirements in terms of part quality can be met in FB coating through the implementation of appropriate process control procedures, as shown in [14]. In FB, the coating build-up of ceramic or, in general, hard material is the result of the repeated impacts of hard and sharp particles on the softer metal substrate. A small portion of the particles remains trapped inside the outermost layers of the impinged metal substrate. The reiteration of these impacts can give rise to the formation of relatively thick (generally, few microns), compact, and dense coatings [15]. Experimental findings showed that tough and well-adhered Al_2O_3 films could be obtained using a fluidized bed of alumina powder. Such films were consistently found to grow by only increasing FB processing time [15]. Furthermore, FB processing was found to cause both the onset of compressive residual stresses in the impinged substrate and an increased hardening level in external layers of processed components, without causing significant erosion/abrasion of the treated surface [16]. As shown in [15], film build-up by FB technique could give rise to the formation of graded properties inside the coating, with the concurrent improvement in mechanical and tribological performance of the Al alloy after the formation of the Al_2O_3 coating on it.

The pertinent literature shows wear resistance and chemical inertness of coated metals could be affected by heat treatment [17–19]. These phenomena are related to grain coarsening and softening of the materials, aspects to take into account also in the case of alumina coatings.

In this context, the present work investigates a thermal post-treatment of Al substrates coated with Al_2O_3 to promote further improvement in the coating properties, due to the diffusion mechanism of alumina promoted by the high temperature of the post-treatment. The effect of the thermal post-treatment temperature and duration on morphology, microstructure, hardness, and scratch resistance of the coatings was analyzed. Wear resistance and chemical inertness of coated and heat-treated Al was also investigated by wear tests and dipping in acid solutions. The results of the characterization tests show the protection grade the coatings were able to provide on aluminum alloys was strictly related to the temperature and duration of the thermal post-treatment, with that being potentially able to increment the overall performance of the Al_2O_3 coatings FB process was found to generate continuous coatings after 200 min, during which Al_2O_3 fragments impact the ductile substrate, deform it, and remain adhered. Coated surfaces showed higher HV than uncoated ones, and maintained high values of HV also after heat treatment at 200 °C. Coating delamination was never observed after indentation, scratch, and wear tests, demonstrating the good adhesion and wear resistance of coatings. A significant improvement of wear resistance was achieved performing heat treatment at 600 °C. At the same time, this condition of heat treatment allowed the increase of chemical inertness.

2 Experimental

2.1 Materials and equipment

Samples 25 × 25 mm^2 in size were obtained from AA 6082T6 rolled sheets, 3 mm thick. After surface cleaning, the samples were submitted to the FB coating process. Al_2O_3 powder with 16 μm average mesh size and 0.67 shape factor (Smyris Abrasivi srl) was pre-loaded in the fluidized bed.

The scheme of the FB system and the steps of coating process used in this work are elsewhere reported [13]. In the present investigation, the samples were clamped on a horizontal shaft rotating at 600 rpm and kept in the inner part of the fluidization column. They were exposed for 200 min to repeated impacts by the incoming alumina powder. The fluidizing gas (air) and the particles were both inert and there were no reactions inside the bed. A uniform coating thickness in the range of 10–15 μm was obtained as a result of the repeated impacts of the hard particles on the softer substrate.

The heat post-treatment performed after FB deposition took place in a convection oven (Nabertherm model P330). The parts of the coatings more susceptible to the thermal transformation are those on top, being this the main reason why a coating with graded properties is generated. The graded coatings consist in outermost layers richer in alumina and innermost layers progressively richer in aluminum. Temperature and time of the heat post-treatment were varied in the range 200–600 °C and 10–240 min, respectively. Table 1 shows the operational conditions tested.

2.2 Characterization

Field emission gun scanning electron microscopy (FEG-SEM Leo, Supra 35, Carl Zeiss SMT, Inc. Thornwood, New York)) was used to take high-resolution images of substrates and coatings.

A contact gauge surface profiler ((TalySurf CLI 2000, Taylor Hobson, Leicester, UK) was used to measure the 3D

Table 1 Experimental plan

Sample	Coating	Heat treatment	
		Temperature, °C	Time, min
1	No	/	/
2	Yes	/	/
3	Yes	200	120
4	Yes	200	240
5	Yes	600	10
6	Yes	600	20

morphology of the as-received and coated substrates, before and after heat post-treatments. Surface profiles with a lateral spacing of 1 μm were recorded. Areas 10×10 mm^2 in size were examined. TalyMap software Release 3.1 was used for data analysis and the evaluation of the roughness parameters.

Depth-sensing micro-indentation (Micro-Combi, CSM Instruments, Peseaux, Switzerland) was used to perform instrumented micro-hardness measurements. Standard micro-hardness tests (micro-Vickers indenter) were performed on coatings and substrate by applying a set of increasing loads, 3, 5, and 10 N, to assess qualitatively the mechanical behavior of the alumina coatings and aluminum alloy under specific loading conditions.

X-ray diffraction (XRD) measurements were carried out by a Philips X'Pert Pro diffractometer, equipped with a plane mono-chromator using Cu Kα radiation (λ = 1.5418 Å).

Adhesion of the coatings to the substrates was assessed by scratch tests. Scratching procedures were carried out by a Rockwell C-type conical indenter with a rounded tip, 100-μm radius, operating in the progressive mode. Sliding pattern 3 mm long were obtained setting the scratch speed at 1 mm/min, and increasing the load from 100 mN to 30 N, at ~ 20 ± 0.2 °C and ~ 40% RH. The magnitude of the residual scratch ditch, R_d, and the extent of immediate recovery, $P_d - R_d$, were evaluated. The tests were repeated three times for each testing condition, and the minimum distance between two adjoining scratches was at least 4 mm to achieve data representative of the average response over a larger surface area. The scratch patterns were visually inspected by FEG-SEM to classify the behavior of the alumina coating submitted to high local stresses, since the applied load is absorbed by the coating or it is transferred to the substrate underneath and different defects can be generated during the scratch tests [20].

Dry "pin-on-disk" tribological tests (Tribometer, C.S.M. Instruments, Peseaux, Switzerland) were used to characterize the wear response of the coated and uncoated substrates. Two Newtons normal load was applied through a stainless steel (100Cr6) spherical counterpart (diameter 6 mm). The length of the wear pattern was 6 mm, the sliding velocity 0.05 m/s

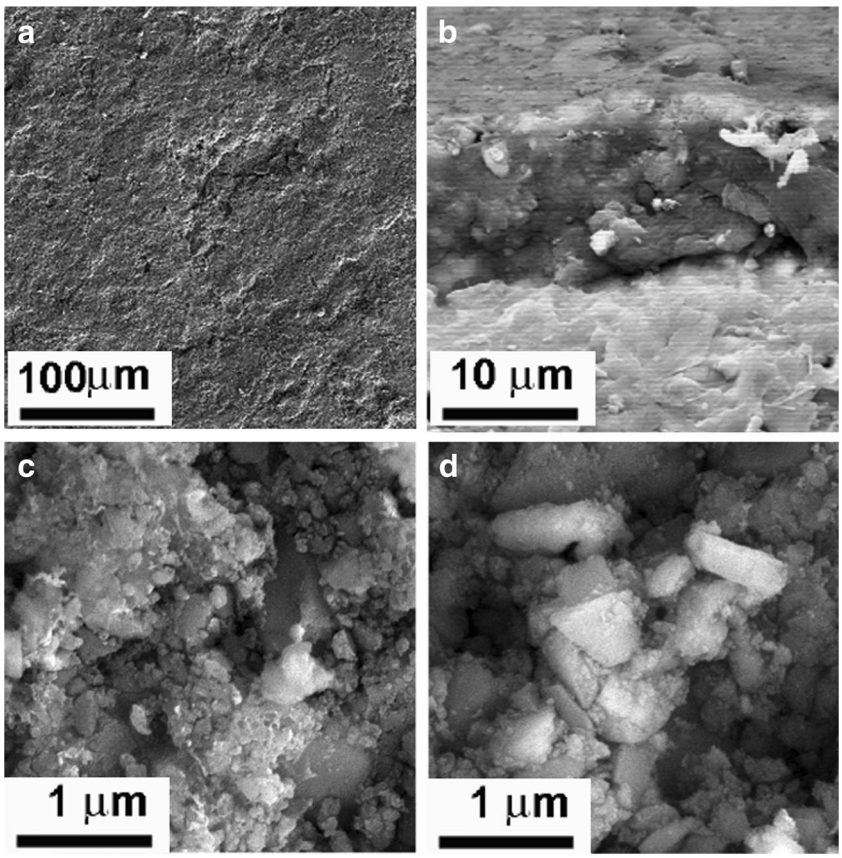

Fig. 1 SEM micrographs: **a** morphology and **b** cross-section of coated sample before heat treatment, **c** morphology after heat treatment at 200 °C 240 min, **d** morphology after heat treatment at 600 °C 20 min

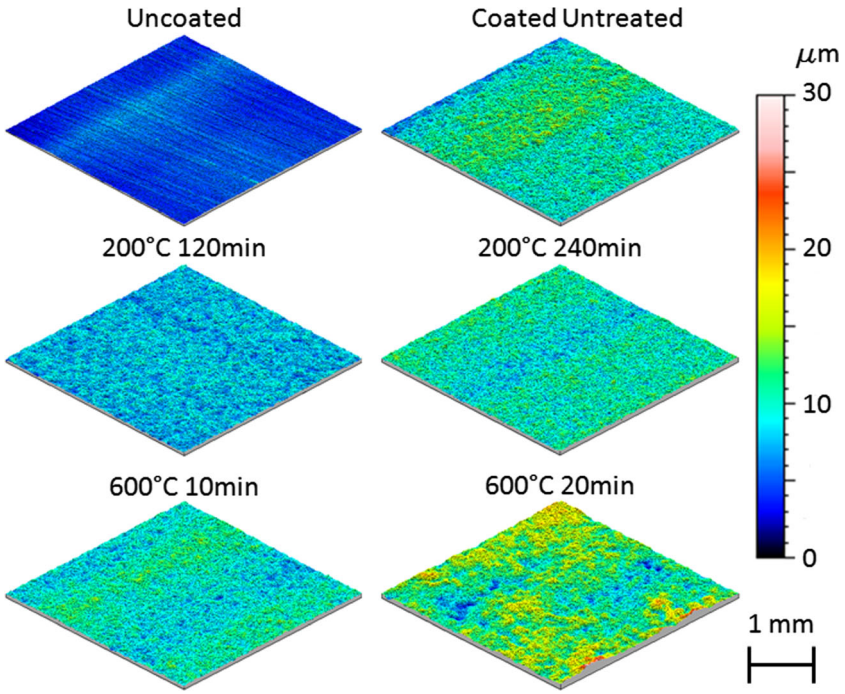

Fig. 2 Profilometry: 3D maps

and the overall sliding distance was set at 5, 10, 20, 60, 180, 500, and 1000 m (1000 m only for sample 6, 500 m only for samples 5 and 6).

Wear response of the coatings was analyzed by the profiler, measuring the 3D morphology of the wear patterns after the tribological tests. Surface profiles with a lateral spacing of 1 μm were recorded to cover the whole area of the patterns. TalyMap software allowed the evaluation of the wear volume. Finally, wear patterns were visually inspected by means of a stereoscope (Nikon).

The grade of protection the coatings are able to ensure was also assessed by accelerated chemical inertness tests. The coated substrates were dipped for 7.5 h in hydrochloric acid (HCl, 0.1%) or sodium hydroxide (NaOH, 0.05%) solutions, at room temperature. The status of the coatings was checked for integrity, taking pictures of the surface every hour. The coating areas removed after tests were evaluated converting images to grayscale, eliminating the hue and saturation and retaining the luminance. Intensity thresholds were then selected based on the image histograms. Specifically, brighter pixels (that are more likely to pertain to corrosion) were set to white. The percentages of brighter corroded areas were estimated by computing the ratio of the white pixels to the image resolution.

3 Results and discussion

During the FB process, the embedding of small and hard Al_2O_3 particles into the softer aluminum substrate and their accumulation promoted the growth of alumina coatings, according to the trend earlier described in [15]. A fast growth of the coating was detected during the first minutes of the FB process, and after 200 min, an almost constant thickness was achieved. For that reason, in the present investigation, the samples were processed by FB for 200 min. The repeated impacts of the incoming alumina powder allowed the

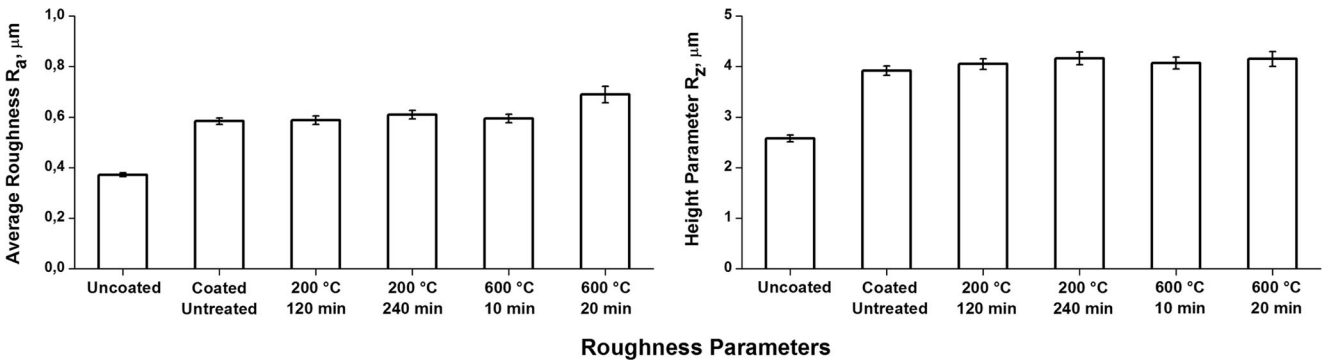

Fig. 3 Profilometry: roughness parameters

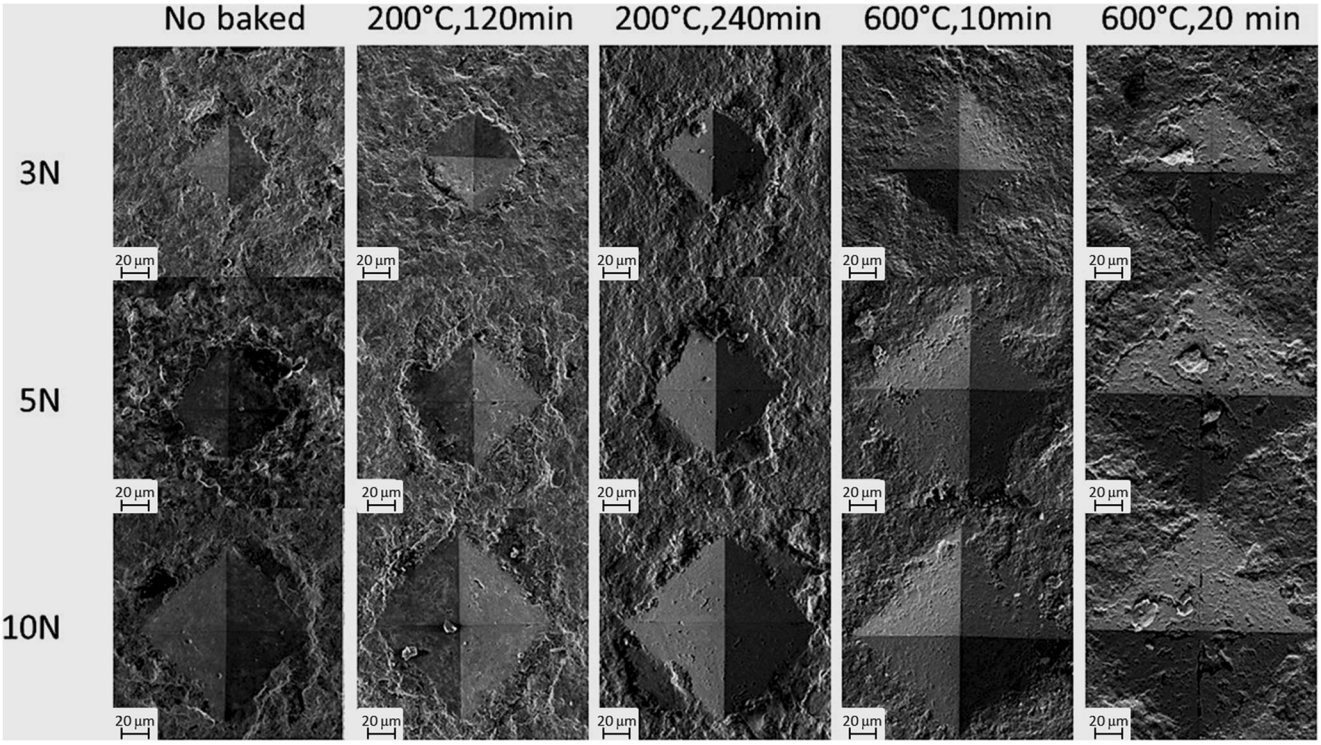

Fig. 4 Vickers micro-hardness tests: micrographs for different loads and post-treatment conditions

achievement of the full coverage of the aluminum substrate with a continuous alumina overlying topcoat. A longer processing time was avoided, since it was found to cause only minor changes in mass growth, due to the saturation of the external layer, and increase the probability to impair the sample surface, generating defects. In fact, if longer processing time is used, incoming Al_2O_3 fragments can impinge on the outermost weakly adhered and hard alumina, causing its removal rather than its consolidation onto the underlying layers. That would only result in partially covered portions of the substrates, according to experimental results in [15].

Fig. 1a shows that the process conditions, herein investigated, allowed the achievement of a homogeneous coating, and coating thicknesses in the range of 10–15 μm was measured (Fig. 1b, the coating is darker than the substrate).

The aspect of the alumina coatings deposited by FB is well different from the one achievable with the other technologies, such as anodization and thermal spraying, as reported in [15]. In particular, defectiveness generated by the FB process was found to be small if compared with defectiveness, which could arise on alumina coatings deposited by anodizing [21] or thermal spraying [12]. The

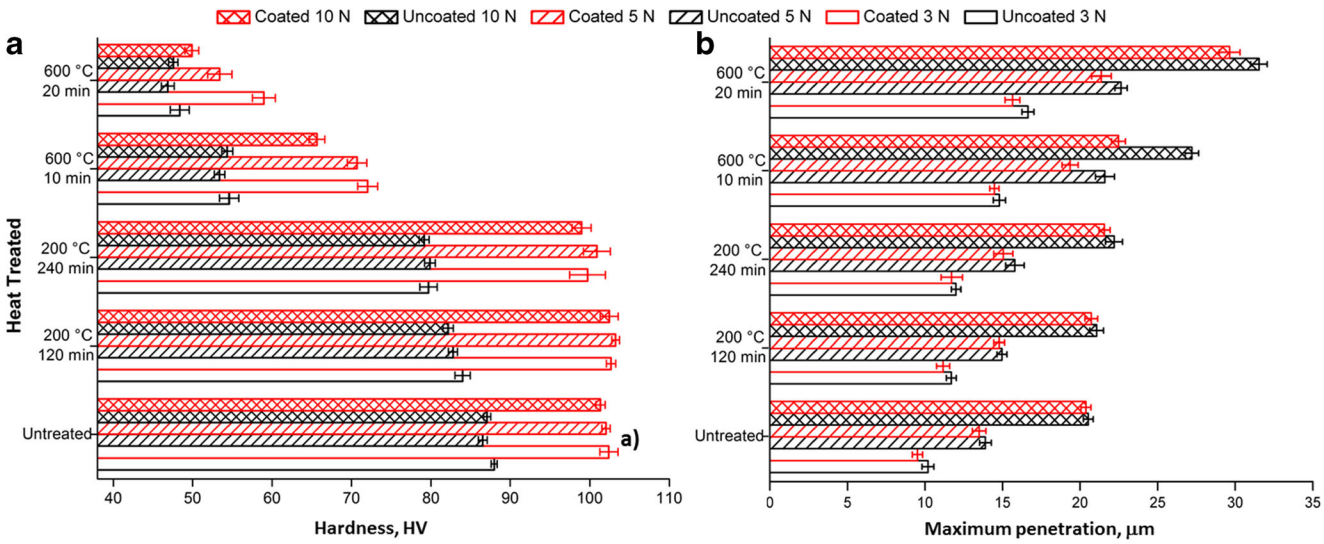

Fig. 5 Vickers micro-hardness tests: **a** HV for different loads and treatment conditions, **b** maximum penetration

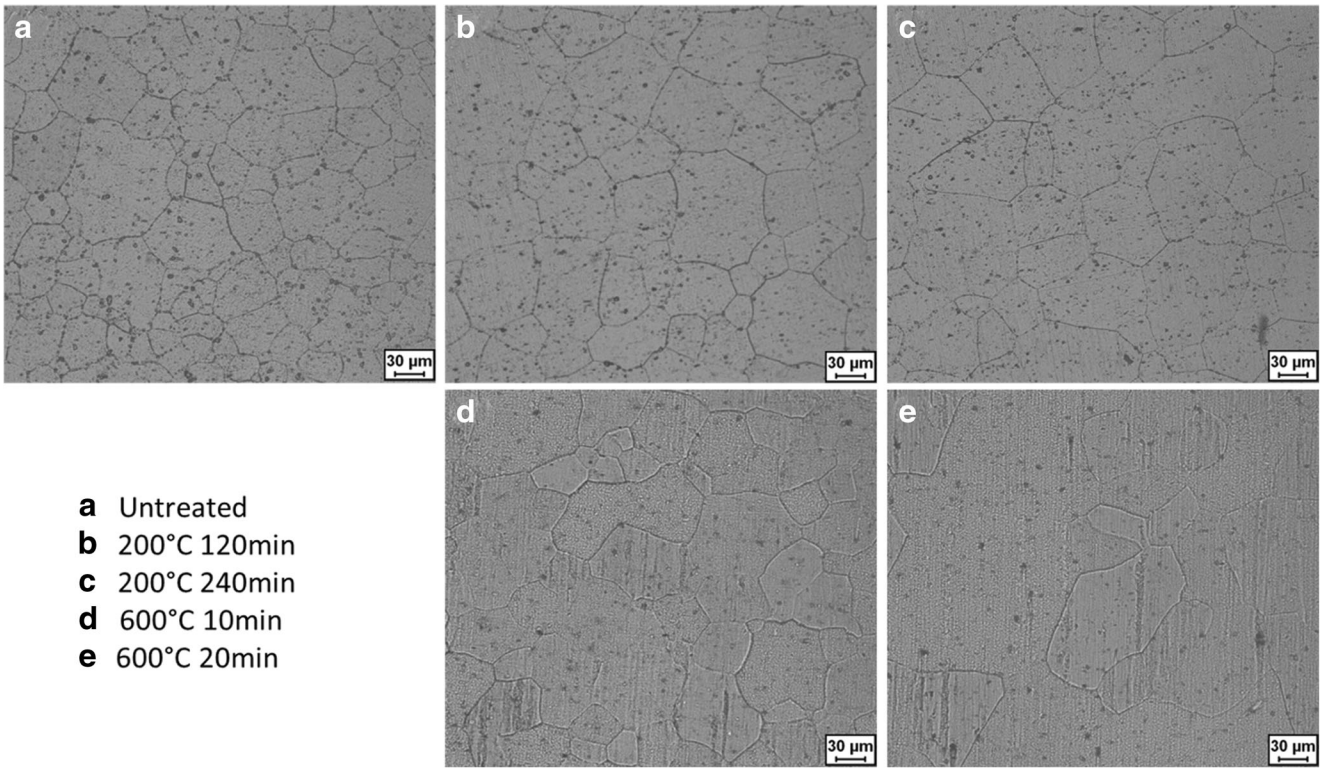

Fig. 6 Al grain size for different treatment conditions

latter processes can lead to Al_2O_3 coatings characterized by the presence of both vertical and transversal cracks (up to 1 μm in width), which might compromise adhesion and wear resistance of the coatings.

Thermal post-treatments of the Al_2O_3 coatings deposited by FB should lead to compact and dense coatings (Fig. 1). After the thermal post-treatment of the FB coatings at the different temperatures, coatings with comparable roughness profiles were achieved whatever was the setting of the post-treatment conditions (Fig. 2).

Figures 2 and 3 show the morphology and roughness parameters of the aluminum substrate and Al_2O_3 coatings, before and after heat post-treatments. Average roughness R_a and ISO 10-point height parameter R_z of the coatings were ~ 0.57–0.76 μm and ~ 3.7–4.5 μm, respectively, higher than those of the uncoated aluminum surface ($R_a < 0.4$ μm and $R_z < 3$ μm). This result is ascribable to the aforementioned coating mechanism according to which Al_2O_3 fragments impinge the ductile Al substrate, deform it, and remain entrapped in the metal, generating, progressively, a corrugated morphology. In addition, the surface morphology depends on the build-up of the Al_2O_3 coatings, that is, by the progressive superimposition of small fragments, which, owing to their geometry, cannot produce smooth surface finishes. However, even after 20 min of heat post-treatment at 600 °C, the thermal post-treatment of the Al_2O_3 particles entrapped on the aluminum substrate

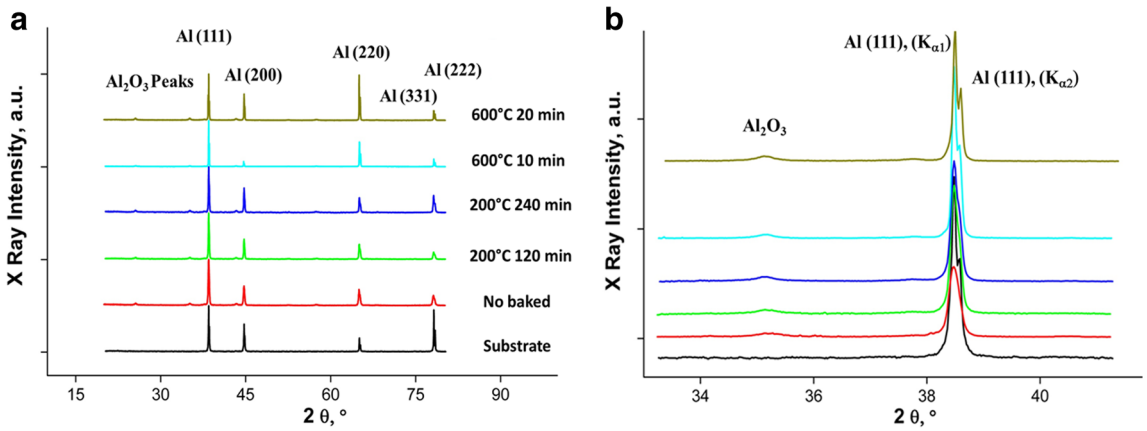

Fig. 7 X-ray diffraction measurement: **a** diffractograms for different treatment conditions, **b** analysis of Al (111) peaks

Table 2 X-ray diffraction measurement: Bragg angle θ, full width at half maximum (FWHM), average micro-strain ε, for different treatment conditions

	θ	FWHM	ε
Not baked	38.48	0.22	$5{,}5 \times 10^{-3}$
200 °C 120 min	38.48	0.19	$4{,}7 \times 10^{-3}$
200 °C 240 min	38.48	0.18	$4{,}5 \times 10^{-3}$
600 °C 10 min	38.48	0.11	$2{,}7 \times 10^{-3}$
600 °C 20 min	38.5	0.08	2×10^{-3}

(Fig. 1d) played a minor role on roughness parameters, with only R_a slightly increasing (Fig. 3).

Figure 4 shows the results of the micro-hardness tests, applying the different loads of 3, 5, and 10 N and using a Vickers indenter. Al_2O_3 coatings were found compliant to the plastic deformation of the ductile aluminum substrates under the pressure of the penetrating indenter. There is no coating delamination. This means that Al2O3 coatings by FB process, both after heat post-treatments or not, did not exhibit the brittle behavior, commonly found for similar films grown by different deposition techniques [10–12]. The analysis of the micrographs in Fig. 4 allowed the evaluation of HV (Fig. 5a). The influence of the substrate must be taken into account, being often the penetration depth higher than the measured thickness of the alumina

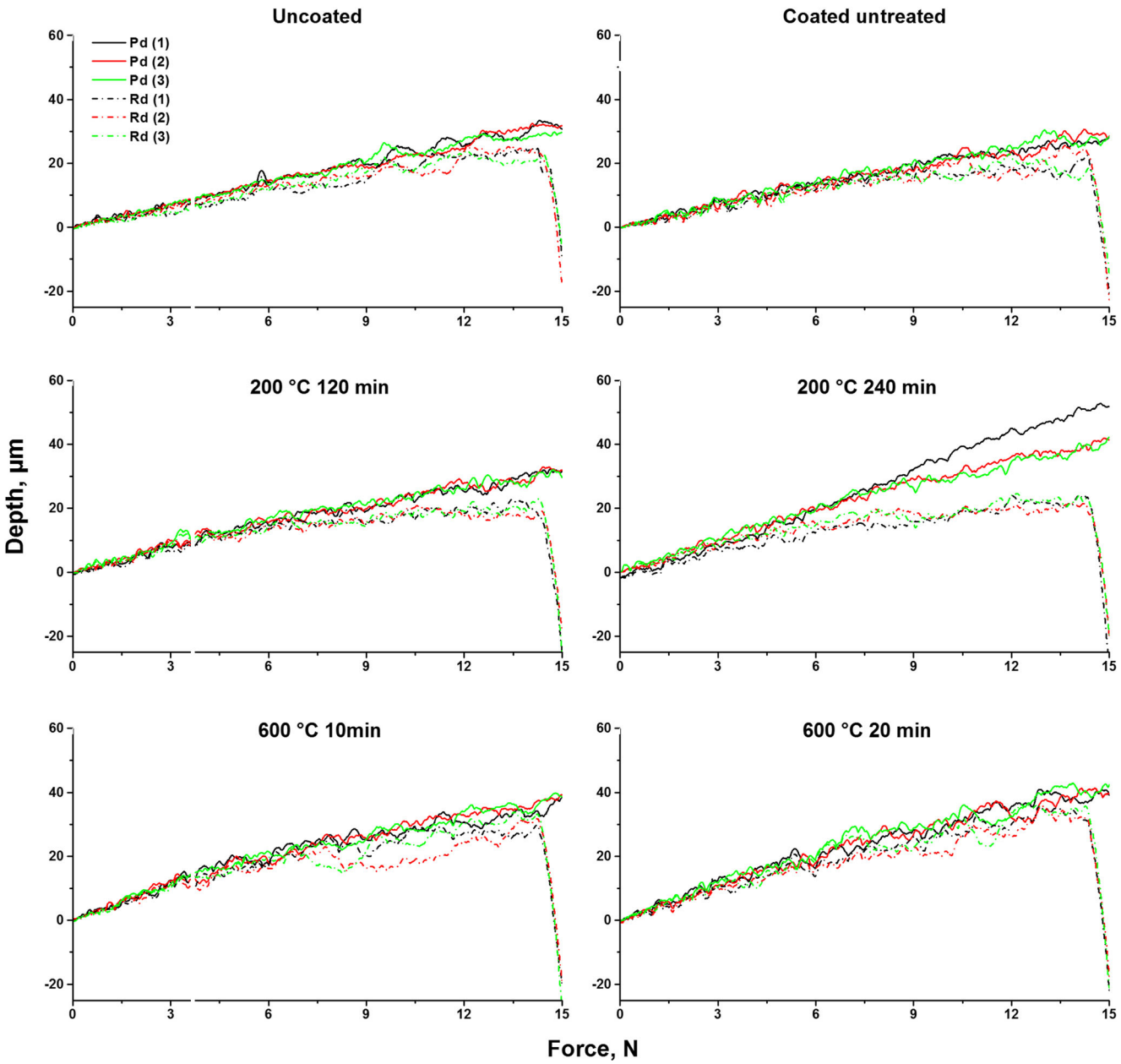

Fig. 8 Progressive load scratch test: penetration (P_d) and residual (R_d) depths

Table 3 Progressive load scratch test: maximum penetration and residual depths, maximum height of front pileup

Sample	Max penetration depth, μm	Residual	
		Max depth, μm	Max height front pileup, μm
Coated, untreated	54.8 + 3.54	37.33 + 0.73	47.41 + 0.72
200 °C 120 min	58.161 + 1.92	38.02 + 3.79	48 + 4.51
200 °C 240 min	62.30 + 6.62	36.34 + 0.34	47.048 + 8.05
600 °C 10 min	64.08 + 0.28	53.04 + 1.88	42.30 + 0.44
600 °C 20 min	73.3 + 0.50	64.7 + 0.78	20.013 + 5.78

layer (10–15 μm), as shown in Fig. 5b. Under these loading conditions, the tests were always affected by the role of the substrate as well as by the effect of the increase in the Al grain size, related to the thermal post-treatment temperature and duration. In particular, some treatment conditions seem to modify the hardness of the resulting system aluminum—alumina.

The peculiar microstructure of the coatings, formed by the continuous superposition of the brittle alumina particles cannot be compared to fully dense film achieved by different technologies (anodizing or others), and thus, its microhardness could be lower. However, coated aluminum always showed hardness higher than crude Al alloy (uncoated), both after thermal post-treatments or not (Fig. 5). Therefore, alumina coatings on aluminum alloys by FB can increase HV of the investigated coating-substrate systems.

Significant variations of HV were not observed after thermal post-treatment at 200 °C, with Al_2O_3-coated Al maintaining high values of HV. In contrast, an increase in thermal post-treatment temperature to 600 °C had negative effects on hardness. That temperature determined a significant decrease in HV, both for coated and uncoated substrates, if compared with samples without thermal post-treatment. This result can be ascribed to the increase in aluminum grain size, being, as said before, the influence of the substrate not negligible (penetration depth higher than coating thickness, Fig. 5b).

The increase of Al grain size according to the thermal treatment conditions can be observed in Fig. 6. It is, in fact, well known how thermal annealing of aluminum alloys cause bigger crystallites in the metal and, in turn, higher ductility and lower hardness, stiffness, and mechanical strength. The trend of the hardness of crude Al according to the temperature of the thermal post-treatment was, as expected, decreasing.

As regards the effect of the loading condition, at 600 °C, a decrease in HV was found increasing the load (from 3 to 10 N). This is ascribable to the graded structure of the coatings (richer in alumina outside and in aluminum inside). Increasing the load, the indenter affects the innermost layer of the coating-to-substrate system, thus measuring lower hardness, especially after thermal post-treatments at very high temperature and for long processing time. A degree of uncertainty in the data of Fig. 5 has to be expected, being the tests performed on as-deposited coatings, presenting irregular morphologies, according to the roughness parameters previously shown.

Figure 7 reports X-ray diffractograms of untreated and treated samples. In particular, Fig. 7a shows the intensity

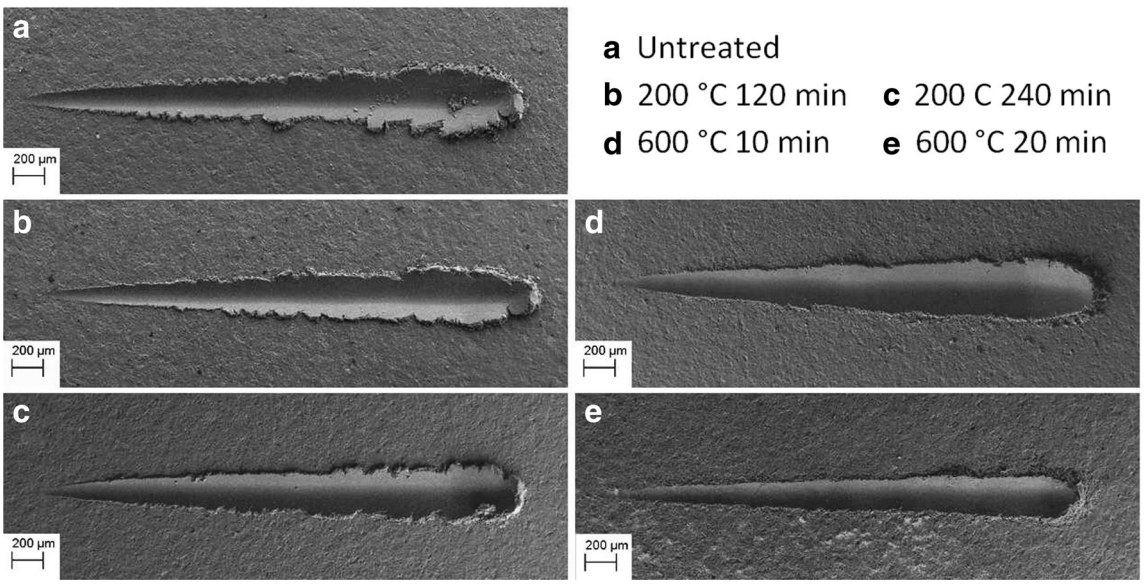

Fig. 9 SEM images of progressive scratch patterns on coated surfaces before (**a**) and after heat treatment in different conditions (**b**–**e**)

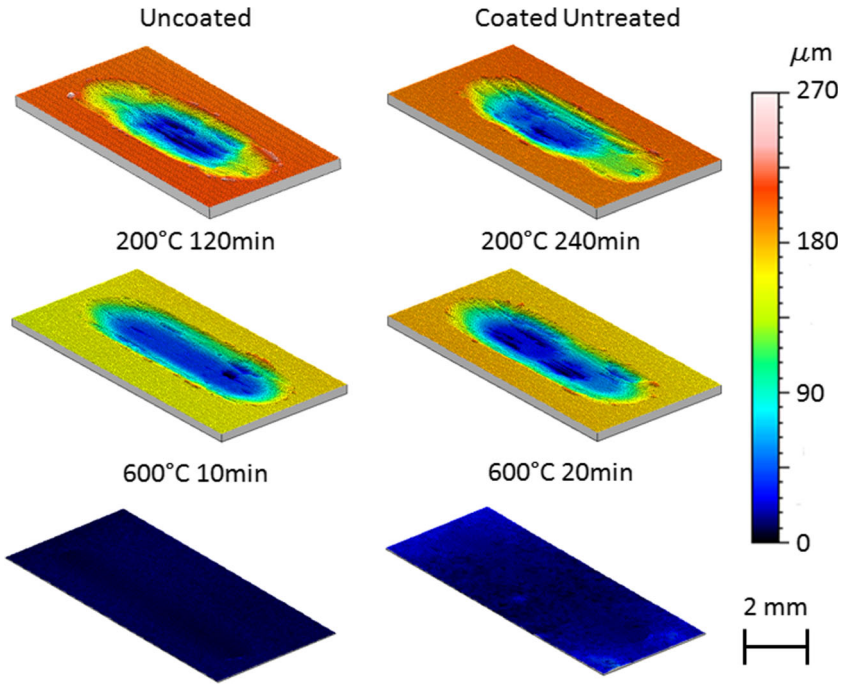

Fig. 10 Wear tests: 3D maps of wear patterns, for 180 m sliding distance 180 m: **a** uncoated; **b** coated, untreated; **c** 200 °C, 120 min; **d** 200 °C, 240 min; **e** 600 °C, 10 min; **f** 600 °C, 20 min

of Al_2O_3 and Al peaks, while Fig. 7b allows to better analyze the peaks related to Al (111). It also allows evaluation of the full width at half maximum (FWHM), which is mainly due to two contributions: the size of coherently diffracting domains and the micro-strains, according to the equations described in [22]. Figure 7b shows in some cases two peaks related to Al (111), $K_{\alpha 1}$ and $K_{\alpha 2}$. They are very close to each other; therefore, an increase of half-

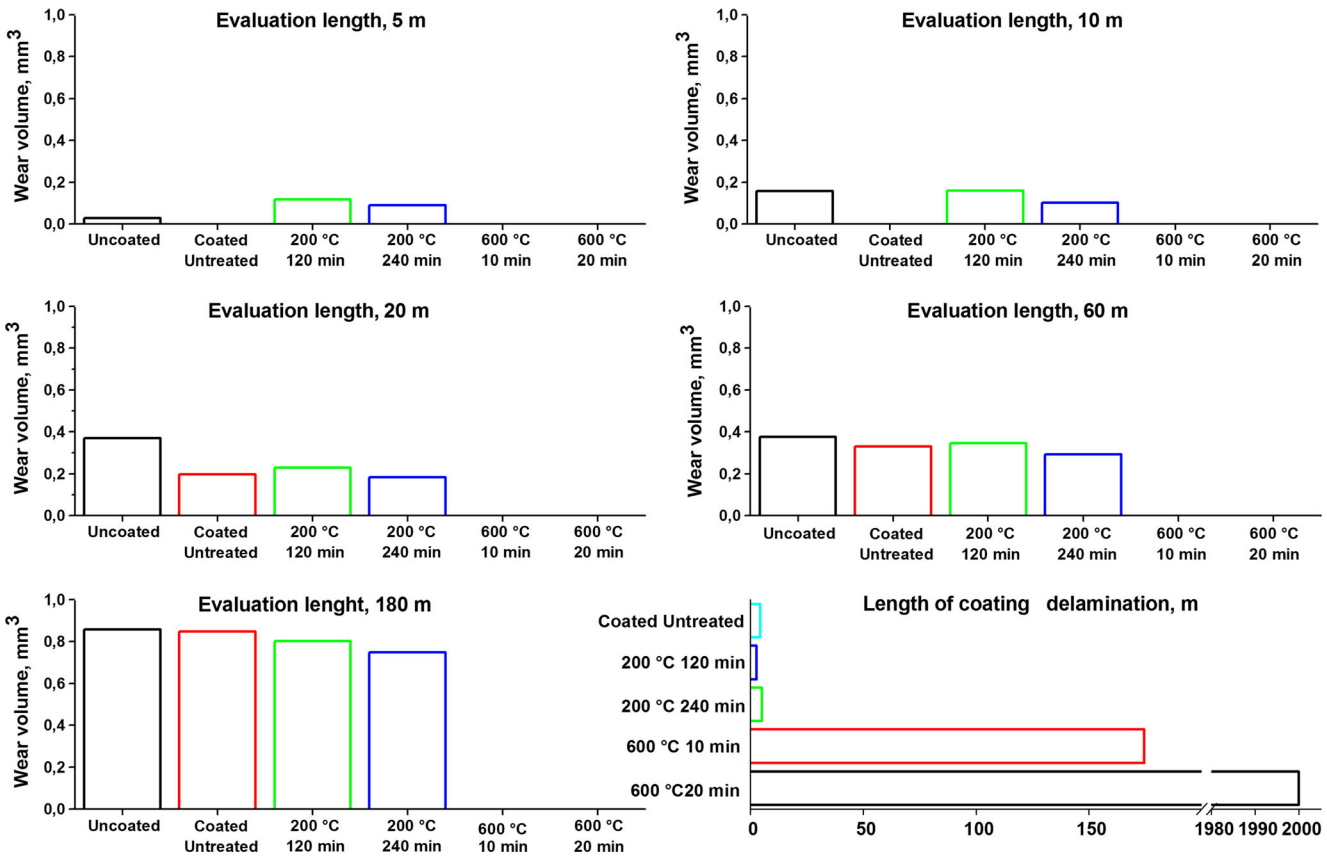

Fig. 11 Wear tests: wear volume at different sliding distance and length for coating delamination

height line width (caused by an increase in grain size or strains) determined the superimposition of the two peaks. When strains were induced by FB and grain size increased it was not possible to distinguish the two peaks. On the contrary, $K_{\alpha 2}$ peak was clearly visible for the substrate and for samples treated at 600 °C. Due to the high treatment temperature (600 °C), the samples underwent a recrystallization, which eliminated the residual stresses induced by the fluidized bed. According to the formulas in [22], the average micro-strain ε can be calculated in different treatment conditions. As Table 2 shows, ε decreases with increasing treatment temperature.

The plots in Fig. 8 allows the comparison of the penetration depth, P_d, and the residual depth, R_d, recorded during the scratch tests. The plot suggests that significant differences in terms of P_d and R_d were not recorded in the presence of Al_2O_3 coatings. However, some significant variations in the scratch performance of the samples were induced by the thermal post-treatments. In particular, higher depths were measured on samples subjected to heat post-treatments at 600 °C. This result is probably ascribable to the increase in Al grain size after thermal post-treatment at high temperature, with such changes being even more apparent for longer processing times. In Table 3, the maximum penetration and residual depths of Fig. 8 are summarized. Both the penetration and residual depths increased by increasing the temperature of the thermal post-treatment. In contrast, the size of the front pileup decreased when 600 °C was set as post-treatment temperature in agreement with SEM images in Fig. 9. After thermal post-treatment at 600 °C, the coating material was not displaced ahead the scratch pattern by the sliding indenter, probably because the improved adhesion between coating and substrate or because the loss of ductility of the alumina coatings, much more firmly adhered to the aluminum substrate.

SEM analysis of the scratch patterns showed neither coating delamination nor initiation and propagation of cracks from the scratch pattern departed whatever the investigated conditions. Fig. 9 shows the SEM images of untreated and post-treated samples. The coated surfaces behave like a semi-ductile metal matrix composite rather than like a brittle ceramic material, according to the graded properties earlier discussed and generated by FB inside the coating [15].

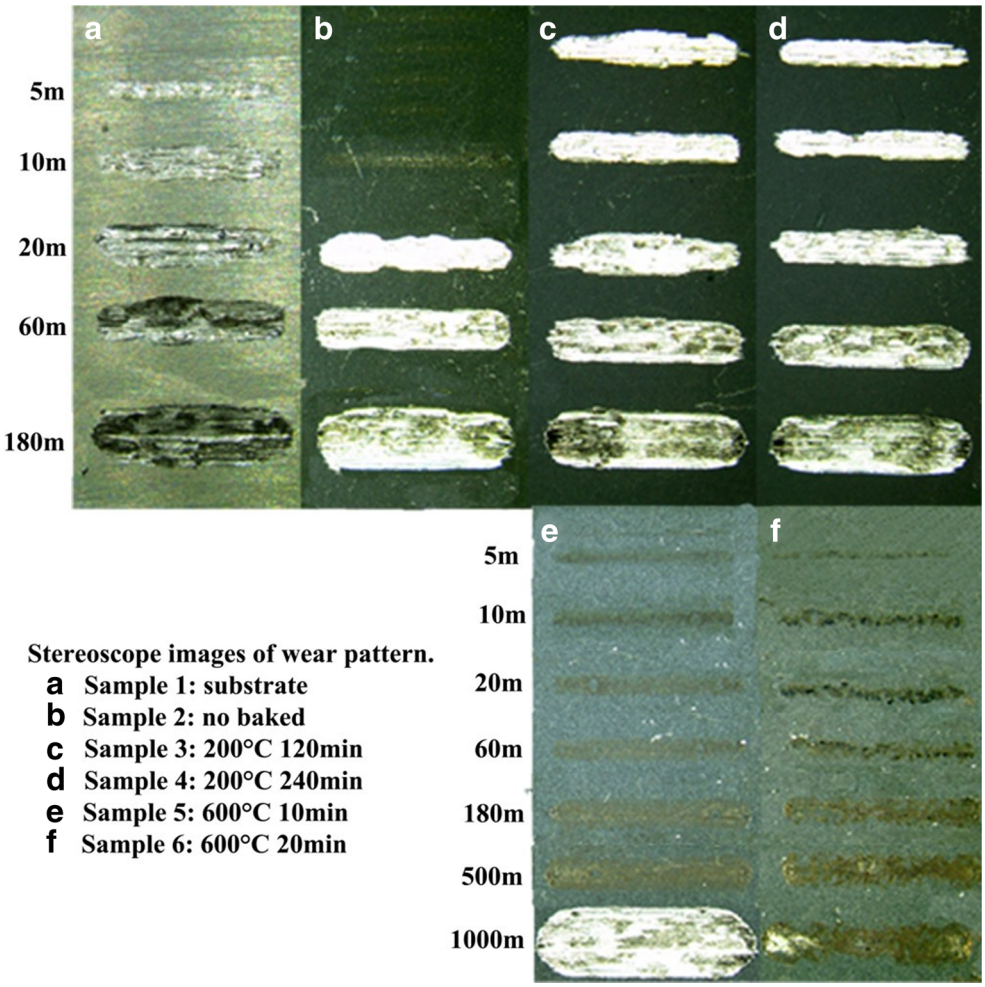

Fig. 12 Stereoscopic images of wear patterns for different sliding distances

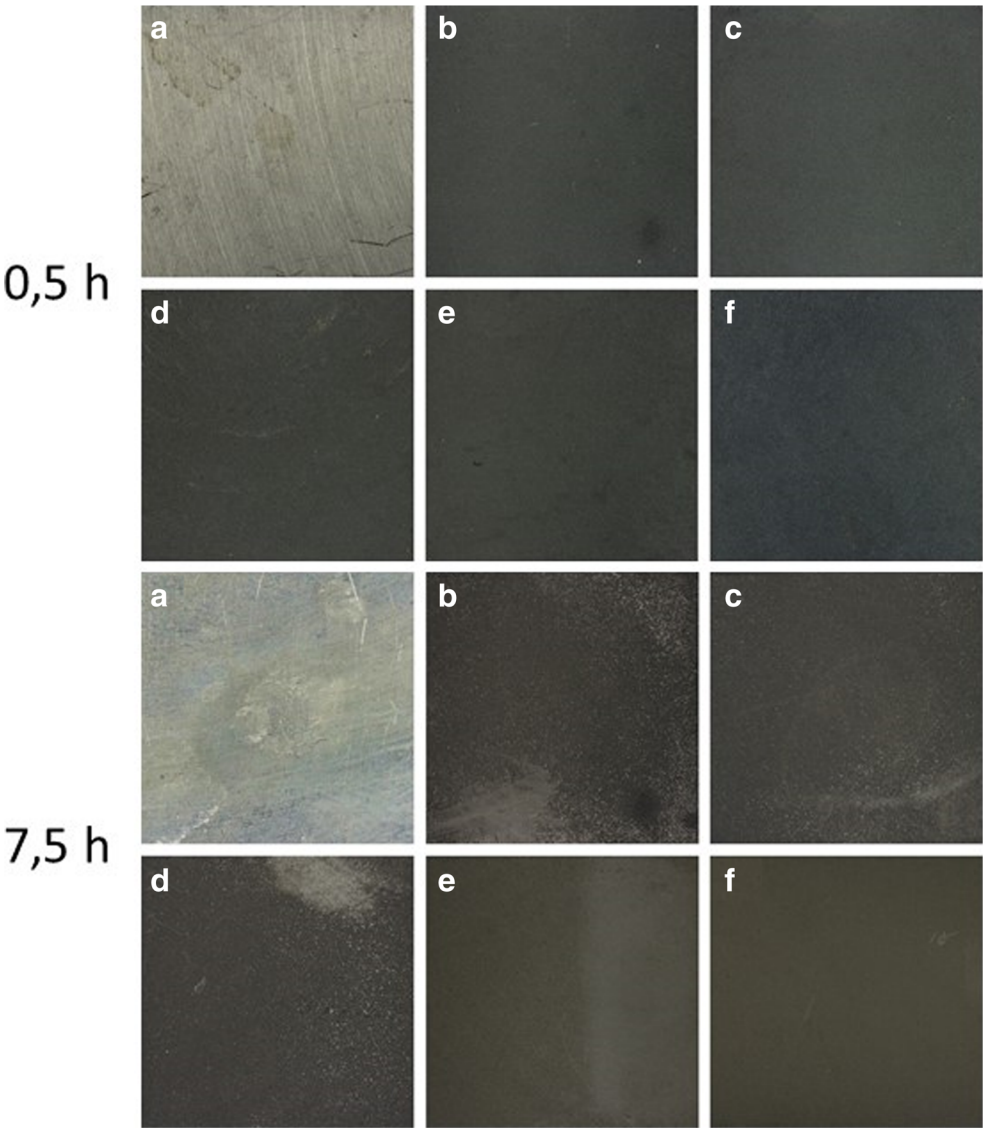

Fig. 13 Images of surfaces after dipping in HCl for 30 min and 7,5 h: **a** uncoated; **b** coated, untreated; **c** 200 °C, 120 min; **d** 200 °C, 240 min; **e** 600 °C, 10 min; **f** 600 °C, 20 min

Regardless of the setting of the thermal post-treatment, a good adhesion between the innermost layers of Al2O3 coatings, rich in Al, and the aluminum substrate was always established.

Scratch resistance of FB-coated samples can be compared with data available on black anodic films deposited on aluminum substrates [6, 23]. A very brittle behavior of anodic films, with coating debris distributed along the whole scratch pattern was found in [23], and critical loads of ~ 7 N were measured on coatings ~ 20 μm thick [6]. In the present investigation, FB-deposited Al_2O_3 coatings, under similar testing conditions, were found to withstand higher scratch loads, up to 30 N, without any formation of residuals after brittle ruptures of the coatings (Fig. 9).

Tribological performance of uncoated, coated, and heat-treated substrates was tested by pin-on-disk, showing that Al_2O_3 coatings may offer an additional protection to erosion/abrasion of the underlying aluminum. A significant effect of the heat post-treatment of the coatings can be also highlighted. The area subjected to tribological test was rebuilt by profilometry (Fig. 10), allowing the evaluation of the abraded volume. Figure 11 shows the trend of the wear volume measured after the tests. The crude aluminum showed the highest abraded volume, confirming the positive effect of FB coating with alumina. Yet, wear resistance can be significantly improved performing heat post-treatment at 600 °C. Samples subjected to treatment at high temperature did not show coating delamination for sliding distance in the range 5–180 m. In particular, Fig. 11e shows the sliding distance the counterpart has to cover before the wear track is visible. The sliding distance approached values that are much higher after thermal post-treatment at 600 °C. The good wear response of the coatings post-treated at 600 °C could be possibly ascribed to their higher coating density and compactness. These properties could be also deduced by the analysis of their scratch response, with the smallest pile-up (i.e., smallest compliance of the coating) being generated by scratching indentations

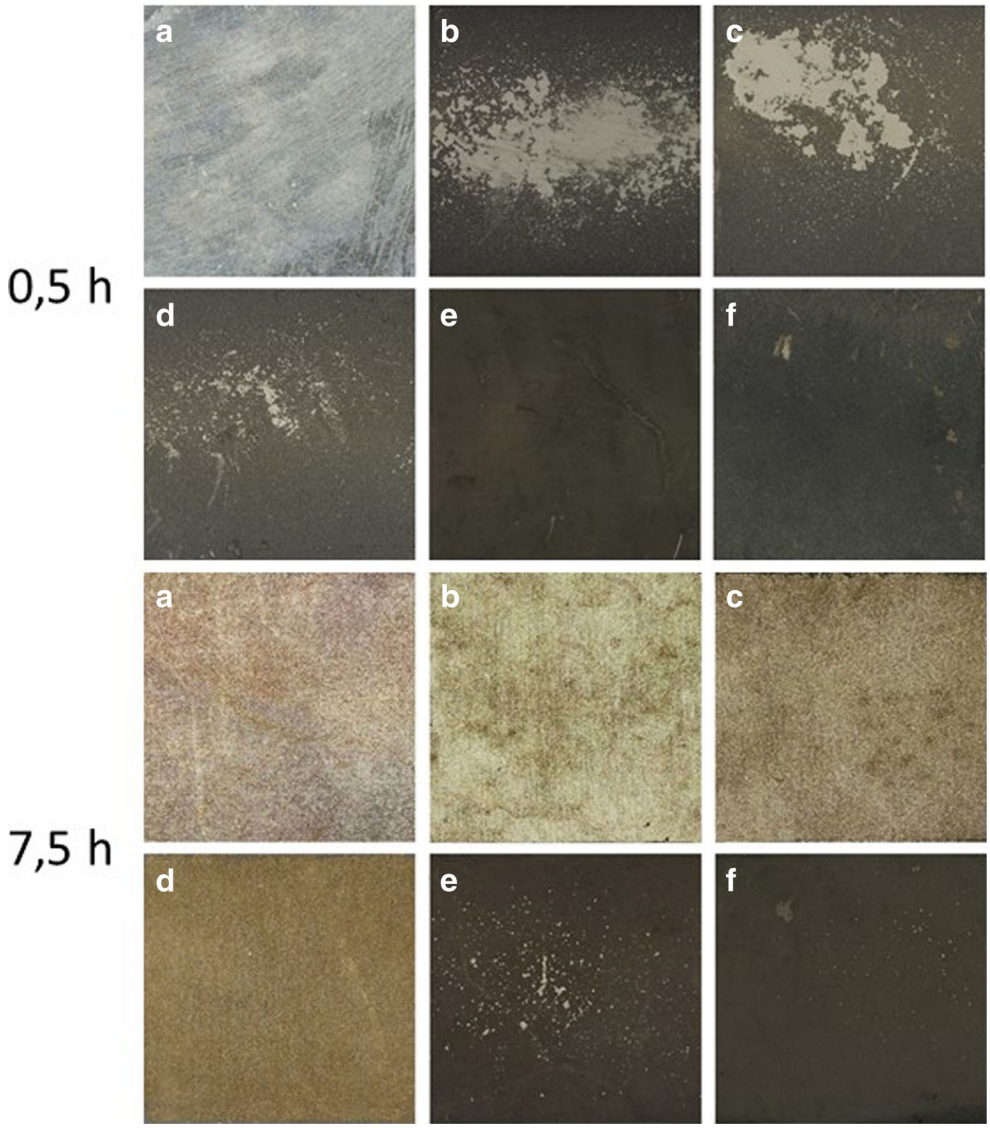

Fig. 14 Images of surfaces after dipping in NaOH for 30 min and 7,5 h: **a** uncoated; **b** coated, untreated; **c** 200 °C, 120 min; **d** 200 °C, 240 min; **e** 600 °C, 10 min; **f** 600 °C, 20 min

performed on coatings post-treated at the highest temperature of 600 °C.

In contrast, the post-treatment temperature of 200 °C did not cause any beneficial effect on wear resistance of the samples. Stereoscopic images in Fig. 12 show the best treatment conditions to obtain significant improvements in wear resistance of the samples, i.e., 600 °C and 20 min.

Although it is difficult to compare wear resistance of Al_2O_3 coatings deposited by FB and those typical of coatings belonging to similar classes (i.e., anodic films on aluminum alloys), it is worthwhile emphasizing how the first ones are able to withstand the action of the counterpart without exhibiting failure up to 180 m sliding distance. In contrast, the anodic films underwent almost instantaneously significant wear, with weight loss by abrasion, even though the very soft loading conditions adopted in [7] (5 N distributed load, 0.0125 N/mm^2 pressure).

Figures 13 and 14 show the performance of the coatings before and after heat post-treatment when dipped in hydrochloric acid (HCl, 0.1%) or sodium hydroxide (NaOH, 0.05%) solutions, respectively, and their comparison with the reference samples (uncoated).

Equations can be found in the pertinent literature to evaluate the corrosion rate of some coated metals, as shown in [24]

Table 4 Chemical resistance: percentage of coating areas removed after dipping in the solutions

Sample	HCl		NaOH	
	0.5 h	7.5 h	0.5 h	7.5 h
Uncoated	100%	100%	100%	100%
Coated, Untreated	0%	15.56%	32,07%	100%
200 °C 120 min	0%	15.23%	22.97%	100%
200 °C 240 min	0%	10.5%	7.48%	100%
600 °C 10 min	0%	0%	0%	2.63%
600 °C 20 min	0%	0%	0%	0.91%

for steel, while, in the present study, the removed areas after corrosion were evaluated by analyzing the images of surfaces. Various degrees of damage were found as a result of the test. The extent of damage related to each condition (coating and heat treatment) is reported in Table 4. As expected, alumina coatings featured better chemical resistance than uncoated surfaces. The latter were found to fail in the first 30 min dipping in both the solutions. A positive effect on chemical resistance was obtained performing heat treatment. The protection grade the coatings are able to provide was strictly related to the temperature and duration of heat post-treatment. In particular, the coatings heat treated at 600 °C for 20 min did not exhibit any visible damage after 7.5 h in both solutions. Lower processing time (10 min) of thermal post-treatment at 600 °C led to small damage when tested in NaOH solution.

4 Conclusions

Al_2O_3 coatings were deposited on aluminum substrates by fluidized bed (FB) technology, and subsequently heat treated under different conditions (treatment temperature and time) to determine a further improvement in the coating performances, according to the mechanism of high-temperature diffusion of alumina. Coatings were characterized in terms of morphology, hardness, chemical inertness, and scratch and wear resistance to evaluate the effect of the thermal post-treatment. The FB process was found to coat aluminum substrates with a tough and well-adherent alumina coating, being the coating thickness in the range 10–15 μm. Surface morphology was found to be affected by the post-treatment temperature, which can cause the increase in Al_2O_3 grain size. The mechanical performances of the coatings were tested by indentation, scratch, and wear tests. Coated surfaces showed higher hardness than uncoated ones, and maintained high values of HV also after heat treatment at 200 °C. A good deformability of coatings was observed under the action of advancing scratching indenter as a result of their graded composition, involving hard Al_2O_3 fragments and ductile Al matrix. Although differences in the scratch performances were induced by the thermal post-treatments, a good adhesion between the innermost layer of coatings and the substrate was established whatever the investigated conditions. Coating delamination was never observed after indentation and scratch tests, demonstrating the good adhesion of coatings. FB-deposited alumina was found to confer additional wear protection to the underlying substrates, and a further improvement in wear resistance was achieved performing heat treatment at 600 °C. At the same time, that post-treatment temperature allowed the increase in chemical inertness of coatings, which did not exhibit any visible damage after 7.5 h dipping in acid solutions.

The experimental findings support the suitability of FB technology, which can be considered a simple, cheap and eco-sustainable method to deposit protective thin layer on aluminum alloys, and show the benefits achievable through thermal post-treatment on coating performances.

References

1. Weiss KD (1997) Paint and coatings: a mature industry in transition. Prog Polym Sci 22:203–245
2. Barletta M, Gisario A, Venettacci S, Trovalusci F (2013) New ways to the manufacturing of pigmented multi-layer protective coatings. Surf Coat Technol 232:860–867
3. Tsipas DN, Anthymidis KG, Flitris Y (2003) Deposition of hard and/or corrosion resistant, single and multielement coatings on ferrous and nonferrous alloys in a fluidized bed reactor. J Mater Process Technol 134:145–152
4. Picas JA, Forn TA, Rilla R, Martín E (2005) HVOF thermal sprayed coatings on aluminium alloys and aluminium matrix composites. Surf Coat Technol 200:1178–1181
5. Takahashi H (2003) Aluminium Anodizing, Corrosion: Fundamentals, Testing, and Protection–ASM Handbook, vol 13A. ASM International, Materials Park, OH, pp 736–740
6. Goueffon Y, Mabru C, Labarrere M, Arurault L, Tonon C, Guigue P (2009) Mechanical behaviour of black anodic films on 7175 aluminium alloy for space applications. Surf Coat Technol 204:1013–1017
7. Bensalah W, Elleuch K, Feki M, De Petris-Wery M, Ayedi HF (2009) Comparative study of mechanical and tribological properties of alumina coatings formed on aluminium in various conditions. Mater Des 30:3731–3737
8. Ding HY, Dai ZD, Skuiry SC, Hui D (2010) Corrosion wear behaviors of micro-arc oxidation coating of Al2O3 on 2024Al in different aqueous environments at fretting contact [J]. Tribol Int 43:868−875
9. Hubert T, Schwarz J, Oertel B (2006) Sol-gel alumina coatings on stainless steel for wear production. J Sol-Gel Sci Technol 38(535): 179–184
10. Mattox DM (1998) Handbook of Physical Vapor Deposition (PVD) Processing
11. Pierson HO (2000) Handbook of chemical vapor deposition. Principles, technology and applications, 2nd edn
12. Crawmer DE (2004) Thermal spray processes. In: Davis JR (ed) Handbook of Thermal spray Technology. ASM International, Materials Park, OH, pp 54–84
13. Barletta M, Guarino S, Rubino G, Trovalusci F, Tagliaferri V (2014) Environmentally friendly wooden-based coatings for thermal insulation: design, manufacturing and performances. Prog Org Coat 77:701–711
14. Trovalusci F, Barletta M, Giannini O. Fuzzy model for electrostatic fluidized bed coating, Proceedings of the 12th Biennial Conference on Engineering Systems Design and Analysis ESDA14, June 25–27, 2014, Copenhagen
15. Barletta M (2010) Al_2O_3 graded coatings on aluminium alloy deposited by the fluidized bed (FB) technique: film formation and mechanical performance. J Eng Mater Technol Trans ASME 132: 310031–3100316
16. Barletta M, Costanza G, Polini R (2006) Al2O3 thin coating of AA 6082 T6 components using a fast regime fluidized bed. Thin Solid Films 515:141–151
17. Dutton R, Wheeler R, Ravichandran KS, An K (2000) Effect of heat treatment on the thermal conductivity of plasma-sprayed thermal barrier coatings. J Therm Spray Technol 9:204–209
18. Novák M, Vojtěch D, Vítů T (2010) Influence of heat treatment on tribological properties of electroless Ni–P and Ni–P–

Al2O3 coatings on Al–Si casting alloy. Appl Surf Sci 256: 2956–2960
19. Al Mangour B, Grzesiak D, Yang J-M (2017) Selective laser melting of TiB2/316L stainless steel composites: the roles of powder preparation and hot isostatic pressing post-treatment. Powder Technol 309:37–48
20. Barletta M, Pezzola S, Trovalusci F, Vesco S (2013) Hard polyurethane coatings on compliant polycarbonate: an application of the 3D deformation response model to scratch visibility. Prog Org Coat 76:1494–1504. https://doi.org/10.1016/j.porgcoat.2013.06.001
21. Tsangaraki-Kaplanoglou I, Theohari S, Dimogerontakis T, Wang Y-M, Kuo H-H, Kia S (2006) Effect of alloy types on the anodizing process of aluminium. Surf Coat Technol 200:2634–2641
22. Deodati P, Donnini R, Montanari R, Testani C (2009) High temperature damping behaviour of Ti6Al4V–SiCf composite. Mater Sci Eng A 521–522:318–321
23. Goueffon Y, Arurault L, Mabru C, Tonon C, Guigue P (2009) Black anodic coatings for space applications: study of the process parameters, characteristics and mechanical properties. J Mater Process Technol 209:5145–5151
24. Al-Mangour B, Mongrain R, Irissou E, Yue S (2013) Improving the strength and corrosion resistance of 316L stainless steel for biomedical applications using cold spray. Surf Coat Technol 216:297–307